Desalination and Water Treatment
www.deswater.com
doi: 10.1080/19443994.2013.852483

53 (2015) 1404–1416
February

Taylor & Francis
Taylor & Francis Group

Waste citrus fruit peels for removal of Hg(II) ions

Tushar J. Sahetya[a], Fuhar Dixit[a], K. Balasubramanian[b,*]

[a]*Department of Ceramic Engineering, Indian Institute of Technology (B.H.U.), Varanasi 221005, India*
[b]*Department of Materials Engineering, Defence Institute of Advanced Technology (DU), Girinagar 411025, India*
Tel. +91 20 24304207/24388835; Fax: +91 20 24389411/24388835; email: balask@diat.ac.in

Received 1 May 2013; Accepted 27 September 2013

ABSTRACT

Mercury is considered as a highly toxic and hazardous pollutant even in trace concentration. Severe consequence of mercury poisoning was observed as Minamata disease in Japan in 1956. Amongst the various techniques used for removal of Hg(II) ions from polluted waters, adsorption demonstrates most promising results. This paper focuses on adsorption of mercury using citrus fruit peels waste from *Phyllanthus emblica* (Indian gooseberry/amla), *Citrus sinensis* (orange), *Mangifera indica* (raw mango) and *Citrus limetta* (sweet lime). The citrus peels were naturally shade dried, powdered to an average particle diameter of 150–200 μ and used without any chemical modification. The impact of solution pH, Hg(II) ion concentration and initial Hg(II) concentration was evaluated in batch adsorption process. The order of Hg(II) adsorption was found to be as: *P. emblica* > *C. sinensis* > *C. limetta* > *M. indica*. Langmuir and Freundlich isotherm describes the equilibrium adsorption condition. The adsorption of Hg(II) followed the pseudo-second-order kinetic mechanism. The thermodynamic investigation showed that the adsorption is a spontaneous process.

Keywords: Mercury; Adsorption; Waste citrus fruit peels

1. Introduction

Mercury is well-known for its exceptional high toxicity from industrial sites to remote corners of the planet [1]. According to USEPA standards, mercury content in drinking water should not exceed 2.0 μg/L [2] and the permitted discharge level of mercury in waste water is 10.0 μg/L [3]. The guidelines by WHO and China [4,5] depicts the inorganic mercury content in drinking water to be 1.0 μg/L. Compared to other heavy metal ions, mercury is highly neurotoxic even at low concentrations [6]. It is also known to cause dysfunction of liver, kidney and gastrointestinal tract [7], narrowing the field of vision and imparting damage to the hearing and speaking ability. High concentration of mercury in water results in Minamata disease, a neurological syndrome first discovered in 1956 in Minamata, Japan. In extreme cases, it can lead to insanity, paralysis and coma and can also affect foetus in womb and even result in death [8–10].

The major sources of mercury pollution are gaseous emission from fossil fuels, chloro-alkali production plants, paint industries, pulp and paper industries, pharmaceutical and cosmetic preparations [11,12] etc. Mercury finds wide application in metallurgy, mirror coating and dental amalgams and as coolant and neutron absorber in nuclear power

---

*Corresponding author.

plants [13]. Mercury also subsists in medical waste and is emitted through medical waste incinerators. The possibility of mercury emissions in the nearby ecosystems exists even with installation of expensive cleaners [13]. Past three decades have experienced the increased emission of mercury from developing nations, offsetting decreased emission from developed nations [14]. Various traditional methods such as chemical precipitation [15], membrane filtration [16], ion exchange [17], lime softening [18], adsorption on activated carbon [19–21], chelate precipitation [22], photo reduction [23,24] etc. have been explored for removal of mercury from water. However, application of such processes is often restricted due to technical and/or economic constraints [25,26] and is limited only for small scale operations and cannot be employed for large water bodies such as rivers or lakes [27]. The use of natural materials like Hoof powder [28], Borassus Flabellifer [29], Lemna powder [5], rice husk [30], tea leaves, coffee beans [31], onion skin [32], waste rubber [33], coconut husk [34], fertilizer waste slurry [35], peanut hull [36], jackfruit peel [37], coir pith [38], flax shive [39] sago waste [40] etc. for uptake of mercury have been reported. However, only few literatures reports are available on the use of unmodified citrus fruit waste peels from Indian gooseberry, mango, lime and orange peel for the removal of Hg from aqueous solutions. These low cost citrus fruits are an attractive and low-cost option for adsorption of mercury ions especially in developing countries like India and Brazil where they are extensively cultivated and mercury pollution is also high [41,42].

The present study demonstrates laboratory analysis on removal of Hg(II) ions from aqueous solutions using the chemically unmodified (raw) peels of citrus fruits like *P. emblica*, *Citrus sinensis*, *Citrus limetta* and *Mangifera indica* as adsorbents. These adsorbents were used in powder form with an average particle size of 150 μm. The adsorption of Hg(II) ions was tested as a function of pH, Hg(II) ion concentration, time and adsorbents used. The equilibrium adsorption isotherms, diffusion mechanism and kinetic mechanisms of Hg(II) adsorption process have also been studied.

2. Materials and methods

Citrus fruit peels were collected from local source, washed and shade dried at room temperature for 7 days. The peels were not sun-dried since the UV rays can affect the active functional groups (like esters). The dried sample were then powdered and sieved below mesh 100 (Tyler standard) [43]. The average particle size chosen was 150 μm. These powdered sorbents were used as such without any further chemical treatment.

Mercury(II) chloride, hydrochloric acid (HCl), sodium hydroxide (NaOH), potassium iodide (KI), zinc sulphate ($ZnSO_4$), sodium salt of EDTA, hexamine (Merck), rhodamine B (Lobachemie) and xylenol orange (Kemphasol) were used as received.

Stock solution of 250 mg/L of $HgCl_2$ was prepared. All the working solutions were prepared by diluting the stock solution using deionized water.

2.1. Adsorption studies

Batch adsorption studies were carried out using 1 g of adsorbent with 50 mL of $HgCl_2$ solution of varying concentrations (25–100 mg/L) at room temperature. Filtration was preferred over ultra-sonication since it loosens the particles adhering to the surfaces and may disrupt or deactivate the biological material. The adsorbents and adsorbates were agitated for predetermined time intervals on a mechanical shaker at 700 rpm after which superntant solution was filtered and used for analysis. The amount of Hg(II) ions in the final 50 mL volume was determined using Nanodrop UV–Visible spectrophotometer (NANO DROP, ND-1000) (calibration plot shown in Fig. 1(a): an average of 3 readings) [44] and verified periodically by titrimetric analysis. The titrimetric determination of mercury was carried out as per the method described in Vogel's textbook of *Quantitative Inorganic Analysis*, Briefly, EDTA titration of mercury using xylenol orange as indicator, hexamine was used as a buffer and the colour change was noted from red to yellow [45].

The amount of Hg(II) ions adsorbed (q) was calculated as follows [21]:

$$q = \frac{(C_o - C_t)}{w} \times V \tag{1}$$

The adsorption efficiency, $Ad\%$ of metal ion was calculated as [21]:

$$\%Ad = \frac{(C_o - C_t)}{C_o} \times 100 \tag{2}$$

where C_o and C_e are the initial and equilibrium Hg(II) ion concentration (mg/L), respectively. V is the volume of the solution (L) and w is the amount of sorbent used (g).

3. Results and discussion

3.1. Effect of pH

The pH dependent adsorption of Hg(II) ions was expressed as percentage of Hg(II) ions adsorbed at various pH values for assorted sorbents used. The results are represented in Fig. 1. It can be observed that adsorption increased with increase in pH, reaching maximum at pH 4. With higher pH values, a slight decrease in the adsorption was noted with all sorbents. According to the stability constant calculations, $HgCl_2$ is the predominant species at pH < 4 is [11,46] in the presence of Cl^- ions, which prevents Hg (II) to bind onto the sorbent at low pH, since chloride ions tend to form more stable complexes with Hg(II) ions such as $HgCl_2$, $HgCl_3^-$, $HgCl_4^{2-}$ [11]. Also, at low pH the excess H^+ ions present in the solution competes with Hg(II) ions for active sites decreasing the adsorption [12]. It was observed that mercury precipitates at higher pH. Hence pH in the range 1–7 was tested. Further, addition of citrus powder to the Hg(II) ions solution was found to lower the pH of the system which is due to the presence of various acid groups present in the adsorbent used.

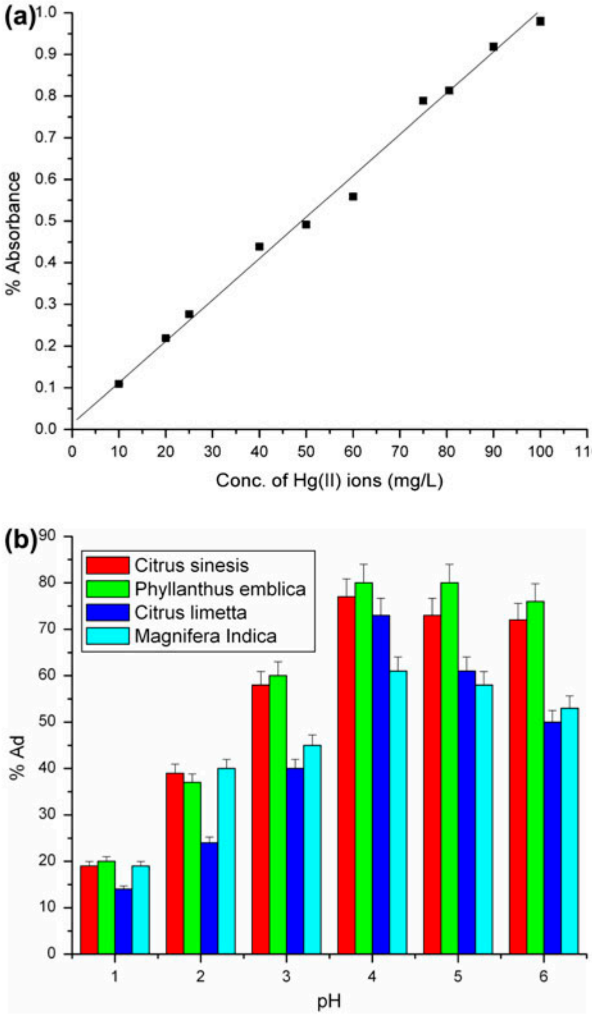

Fig. 1. (a) Calibration curve for Hg(II) ions detection and (b) adsorption of Hg(II) at different pH.

3.2. Adsorption isotherms

Adsorption isotherms are significant to describe the adsorption mechanism, design the adsorption process and test the efficiency of adsorption. The adsorption isotherm indicates the distribution of adsorbent between the liquid and the solid phases at equilibrium state. The isotherms render certain constants whose value articulates surface properties and affinity of adsorbent. Several adsorption isotherms are followed to correlate equilibrium adsorption; well-known isotherms are Freundlich, Langmuir, Temkin, Redlich–Paterson, Dubinin–Rudushkevich and Sips equation [47]. In this study, the equilibrium experimental data for adsorbed Hg(II) ions onto *P. emblica*, *C. sinensis*, *C. limetta* and *M. indica* fruit peels were analysed using the Langmuir, Freundlich, Temkin and Dubinin–Rudushkevich models. The isotherm constants for the four models were obtained by linear regression methods and are presented in Table 1.

3.2.1. Langmuir isotherm model

The Langmuir model assumes monomolecular layer adsorption without any interaction between the adsorbed molecules [48]. It is applicable to homogeneous adsorption where the adsorption of each molecule has equal sorption activation energy [49]. The basic assumption of the Langmuir theory is that the uptake of metal ions occurs on a homogeneous surface by monolayer adsorption without any interaction between the adsorbed ions [50]. The Langmuir model can be represented as:

$$q_e = \frac{q_{\max} \times K_L \times C_e}{1 + (K_L \times C_e)} \tag{3}$$

where C_e and q_e are the equilibrium concentration (mg/L) and amount of Hg(II) ions adsorbed (mg/g), $q_{\max}$ is q_e for a complete monolayer (mg/g), K_L is a constant related to the affinity of the binding sites (L/mg). The linearized form of the Langmuir equation is:

$$\frac{C_e}{q_e} = \frac{1}{q_{\max} \times K_L} + \frac{C_e}{q_{\max}} \tag{4}$$

The Langmuir constants $q_{\max}$ and K_L were obtained by linear regression method. The essential features of Langmuir isotherm is expressed in terms of

Table 1
Equilibrium isotherm data

Adsorption isotherm	Isotherm parameters	*Phyllanthus emblica*	*Citrus sinensis*	*Citrus limetta*	*Mangifera indica*
Freundlich	K_F	0.42	12.32	4.81	2.81
	n	0.3	0.7	0.5	0.5
	R^2	0.9931	0.9969	0.9936	0.9910
Langmuir	q_{max}	285.71	1012.65	840.33	746.62
	K_L	14.16	46.63	372.44	45.15
	$R_L \times 10^{-4}$	7.05	2.14	0.27	2.21
	R^2	0.9386	0.9021	0.9993	0.8991
Temkin	$b_T \times 10^{-3}$	2.51	7.12	5.21	5.51
	a_T	0.1571	0.1367	0.1335	0.1039
	b_T	934.50	347.83	475.34	449.06
	R^2	0.9971	0.9961	0.9857	0.9684
Dubinin–Radushkevich	q_{max}	4354.65	1702.37	1472.76	1750.45
	K	26.24	43.65	43.03	29.11
	R^2	0.9782	0.9867	0.9151	0.9492

dimensionless constant equilibrium parameter, R_L defined by Hall et al. [51] as:

$$R_L = \frac{1}{1 + (K_L \times C_o)} \tag{5}$$

where K_L (L/mg) is the Langmuir constant. The calculated values of the dimensionless factor R_L are included in Table 1. The R_L value obtained for all the adsorbents are in the range 0–1 which indicates favorable adsorption. The regression coefficient gives good fit with the experimental data for all substrates indicating that equilibrium isotherms can be well described by the Langmuir model.

3.2.2. Freundlich isotherm model

Freundlich equation states that heat of adsorption decreases in magnitude with increase in the extent of adsorption [52]. The Freundlich isotherm assumes that the adsorption process occurs on heterogeneous surfaces and adsorption capacity is related to the concentration of the metal ions at equilibrium. This isotherm model is defined by the equation [53] below:

$$q_e = K_F \times C_e^n \tag{6}$$

where K_F and n are the Freundlich constants related to adsorption capacity and intensity, respectively. The linearized form of this equation is written as:

$$\ln q_e = \frac{1}{n} \ln C_e + \ln K_F \tag{7}$$

Maximum sorption capacity can be calculated from initial concentration C_o and variable weights of sorbent, thus ln q_m is the extrapolated value of ln q for $C = C_o$ [54]. The linear plot of ln q_e vs. ln C_e yields slope of value $1/n$ and an intercept ln K_F [55]. With $C_e = 1$, ln K_F = ln q_e. Favorable adsorption tends to give Freundlich constant "n" value between 1 and 10. Larger value of n indicates strong interaction between adsorbent and adsorbate, while $1/n$ equal to 1 indicates linear adsorption with identical adsorption energies for all the sites. It can be observed from Table 1 that the adsorption of Hg(II) yields positive value of n which are in the range of 0.3–0.7 indicating weak interactions between adsorbent and Hg(II) ions. The high values for the regression coefficients obtained for all systems indicate that the equilibrium adsorption isotherm can also be described by the Freundlich model.

3.2.3. Temkin isotherm model

Temkin isotherm considers that heat of adsorption decreases linearly with coverage of adsorbate–adsorbent interactions [56], adsorption of adsorbate is uniformly distributed [57] and decrease in the heat of adsorption is linear rather than logarithmic as implied in the Freundlich equation. The Temkin isotherm has been used in the form as follows [58]:

$$q_e = \frac{RT}{b_T} \times \ln(a_T \times C_e) + \frac{RT}{b_T} \times \ln C_e \tag{8}$$

where R is gas constant 8.314×10^{-3} kJ mol^{-1} K^{-1}, T is absolute temperature K, b_T is the Temkin constant related to the heat of adsorption (kJ mol^{-1}) and a_T is the equilibrium binding constant corresponding to the maximum binding energy (L/g).

The adsorption data analysed according to Eq. (4) gives linear plots of q_e vs. ln C_e. Typical bonding energy range for ion exchange mechanism is reported to be in the range of 8–16 kJ mol^{-1} while physisorption processes are reported to have adsorption energies less than −40 kJ mol^{-1} [58].

The Temkin constants given in Table 1 suggest that the adsorption involves chemisorption of Hg(II) ions with a satisfactory linear fit data and R^2 value ~0.99 indicating uniform adsorption.

3.2.4. Dubinin–Radushkevich (D–R) isotherm

Dubinin [58] suggested the isotherm to estimate the mean free energy of adsorption. The linearized equation is given as:

$$\ln q_e = \ln q_{\max} - K\left[RT\ln\left(1+\frac{1}{C_e}\right)\right]^2 \tag{9}$$

where K (mol^2 kJ^{-2}) is a constant related to the mean adsorption energy. The plot of ln q_e vs. ln $(1 + 1/C_e)^2$ yields the constant K and $q_{\max}$. The adsorption of Hg (II) ions fits well with the D–R isotherm with regression coefficient values ~0.97.

The overall results indicate that the Langmuir isotherm, Freundlich isotherm, Temkin isotherm and D–R isotherm fit well for all the adsorbent systems as can be seen from Fig. 2, while the equilibrium adsorption can be best explained by Langmuir model which explains that the process of adsorption is physico-chemical involving the thiamine (–S–H) and carboxyl (–COOH) groups of the adsorbent systems.

3.4. Kinetic studies

Adsorption kinetics has been thoroughly studied to investigate the mechanism of adsorption and the rate determining step. Several kinetic models such as pseudo-first-order, pseudo-second-order, Elovich and intraparticle diffusion models have been examined for defining the rate determining step and mechanism of adsorption.

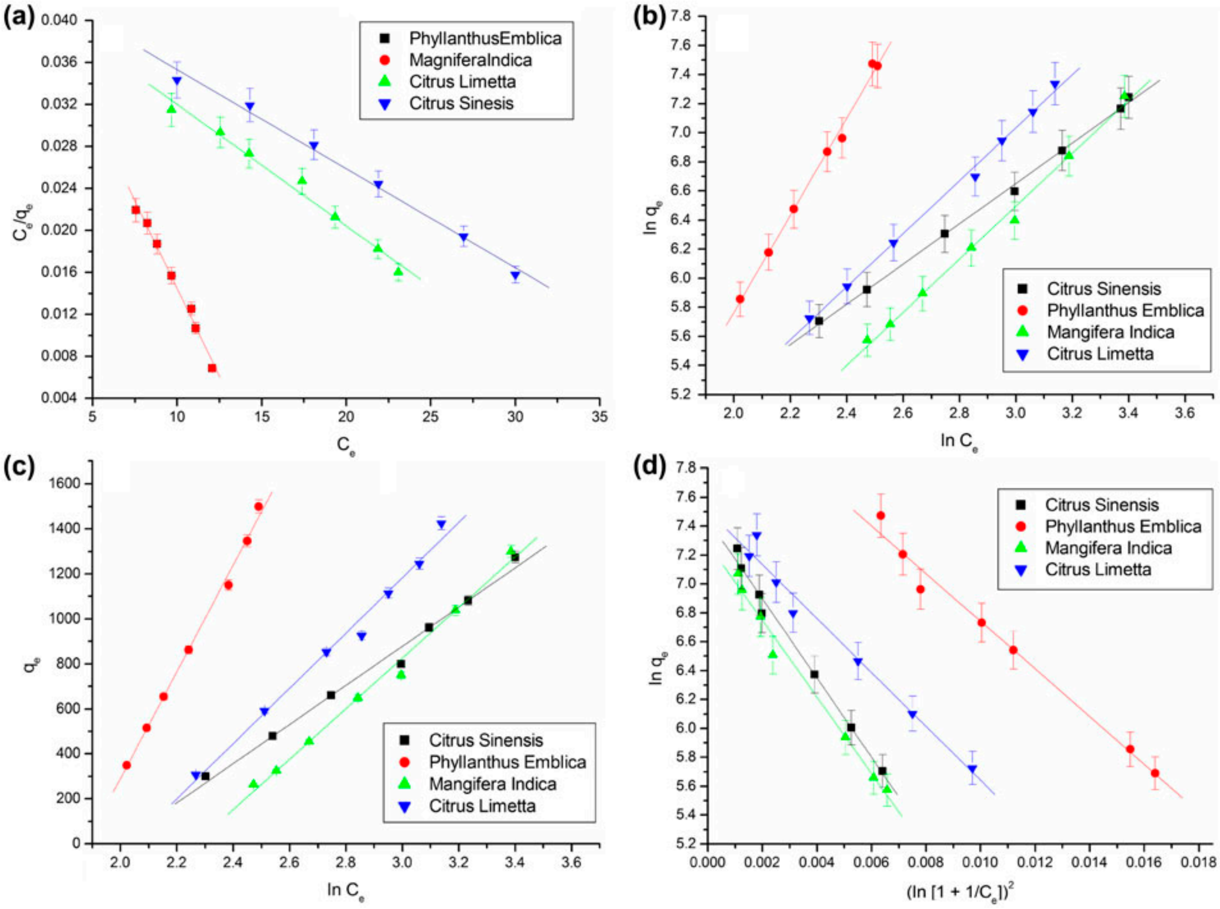

Fig. 2. Adsorption isotherm (a) Langmuir, (b) Freundlich, (c) Temkin, (d) D–R.

3.4.1. *Pseudo-second-order*

The pseudo-second-order reaction considers that the rate is directly proportional to the number of active surface sites present on the adsorbent surface [59]. The pseudo-second-order equation is given as:

$$\frac{t}{q_t} = \frac{1}{k_2 \times q_e} + \frac{t}{q_e} \tag{10}$$

where k_2 ($\text{g}\,\text{mg}^{-1}\,\text{min}^{-1}$) is the pseudo-second-order rate constant. The initial sorption rate:

$$h = k_2 \times q_e^2 \tag{11}$$

The plots of t/q_t vs. t for Hg(II) sorption are linear (Fig. 3) with high correlation coefficients values, R^2 (Table 2). This shows that the adsorption of Hg(II) fits very well with pseudo-second-order kinetic model.

3.4.2. *Pseudo-first-order*

Lagergren demonstrated that the rate of adsorption of solute on the adsorbent depends on the adsorption capacity and follows the pseudo-first-order equation used to estimate the k_{ad}, the mass transfer coefficient. The pseudo-first-order rate equation is given as [60]:

$$\log(q_e - q_t) = \log q_e - \left(\frac{k_1}{2.303}\right) \times t \tag{12}$$

where q_e and q_t are the amounts of adsorbed Hg(II) ions on the adsorbent at equilibrium and at time t respectively (mg/g), and k_1 is the first-order adsorption rate constant (min^{-1}). The calculated values of the pseudo-first-order rate equation are given in Table 2. The straight line with negative slope (Fig. 4) suggests the applicability of this kinetic model.

3.4.3. *Elovich model*

In reactions where adsorption occurs without desorption of products, adsorption rate decreases with time due to increased surface coverage. Elovich equation is considered to be the best models for describing such "activated" sorption [61]. Elovich equation is based on the adsorption capacity describing the

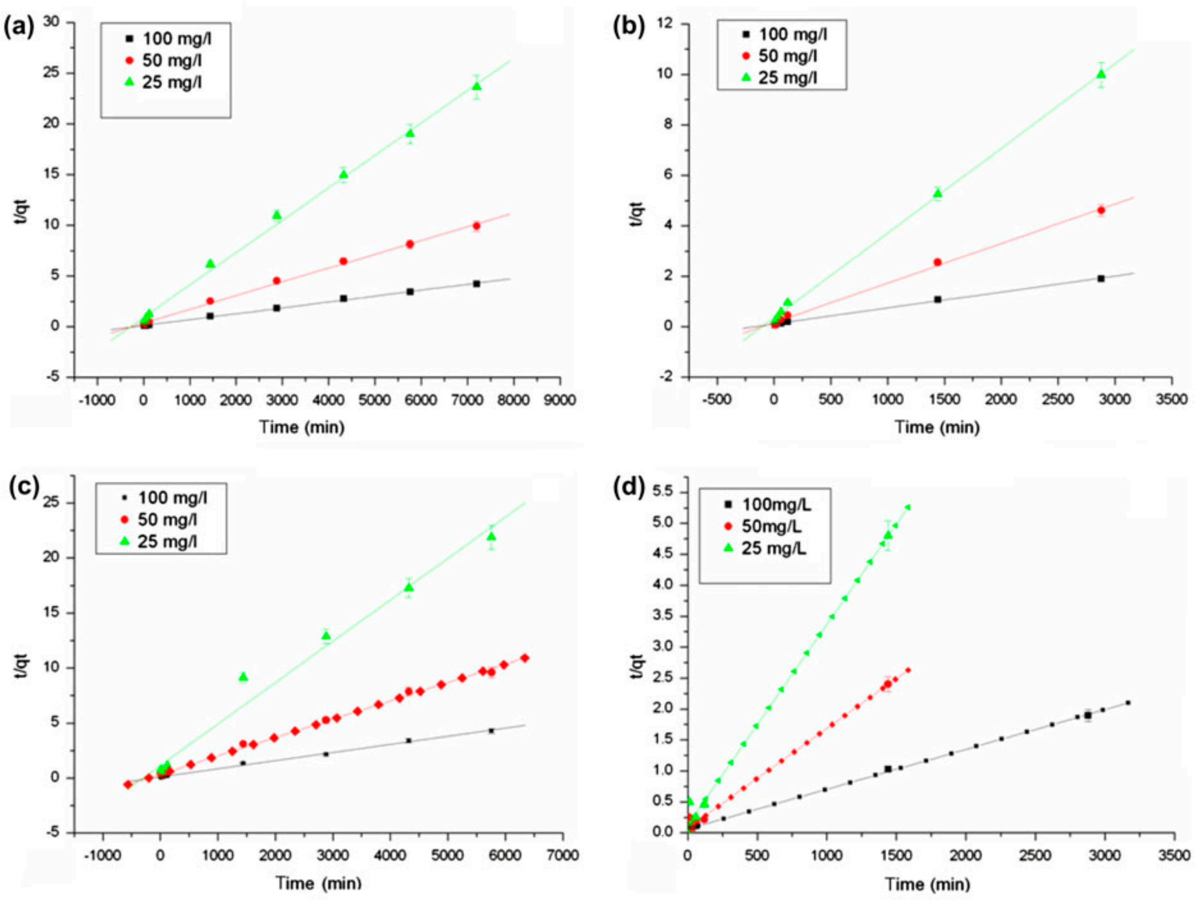

Fig. 3. Pseudo second-order kinetics graphs for (a) *Phyllanthus emblica*, (b) *Mangifera indica*, (c) *Citrus limetta*, (d) *Citrus sinensis*.

Table 2
Kinetics parameters for pseudo first and pseudo second order models

		Pseudo second order			Pseudo first order		
Adsorbents	Con. mg/L	q_e	$k_2 \times 10^{-6}$	R^2	q_e	k_1	R^2
Phyllanthus emblica	100	18.30	689.90	0.9982	24.49	0.0795	0.9945
	50	725.21	5.22	0.9975	17.10	0.0692	0.9942
	25	312.53	11.14	0.9972	12.25	0.0625	0.9978
Citrus limetta	100	8.52	120.66	0.9972	22.82	0.1648	0.9799
	50	636.94	14.46	0.9972	14.99	0.1267	0.9994
	25	297.61	31.47	0.9989	10.82	0.1275	0.9987
Mangifera indica	100	7.29	177.78	0.9965	22.19	0.0948	0.9955
	50	598.80	7.70	0.9958	15.25	0.0999	0.9912
	25	265.95	12.23	0.9812	10.76	0.1241	0.9932
Citrus sinensis	100	8.37	568.84	0.9987	25.25	0.0201	0.9964
	50	621.11	35.053	0.9960	16.42	0.0226	0.9969
	25	446.42	22.18	0.9974	10.92	0.1704	0.9949

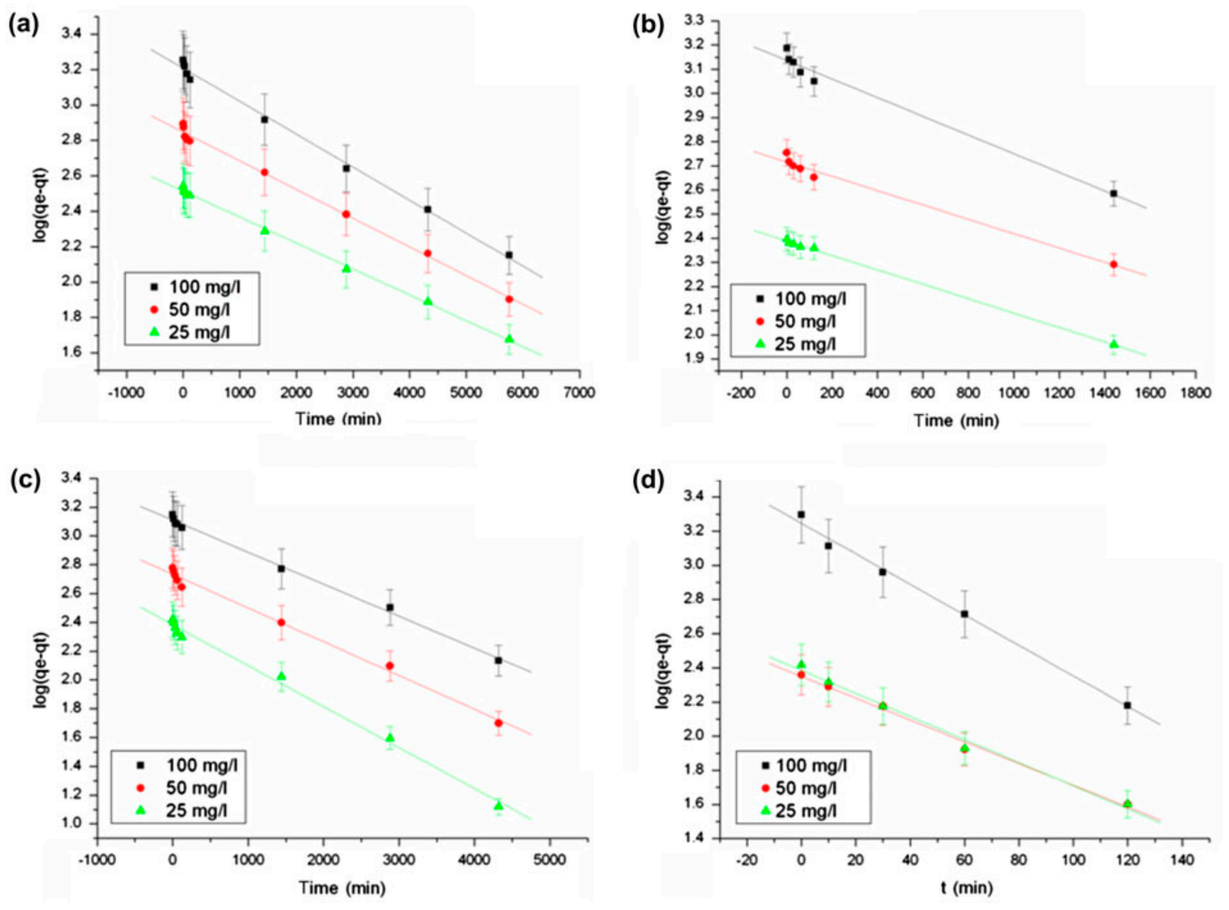

Fig. 4. Pseudo first-order kinetics graphs for (a) *Phyllanthus emblica*, (b) *Mangifera indica*, (c) *Citrus limetta*, (d) *Citrus sinensis*.

adsorption on highly heterogeneous adsorbent, expressed as [62]

$$q_t = \left(\frac{1}{\sigma}\right)\ln(\theta_\sigma) + \left(\frac{1}{\sigma}\right)\ln t \tag{13}$$

Assuming $\theta_\sigma \gg t$ and $q_t = 0$ at $t = 0$.

The results indicate good correlation between the experimental data and theoretical model (Fig. 5) with R^2 value ranging between 0.98 and 0.99 suggesting the applicability of this model for adsorption of Hg(II) on all the four sorbents.

3.4.4. Adsorption mechanism

The prediction of rate-limiting step is a significant factor in adsorption process [63] which is governed by adsorption mechanism. For a solid–liquid adsorption process, the solute transfer is usually characterized by external mass transfer (boundary layer diffusion) or intraparticle diffusion, or both. According to Weber and Morris [64], an intraparticle diffusion coefficient K_{int} is given by the equation:

$$q_t = K_{\text{int}} \times t^{1/2} \tag{14}$$

where K_{int} is the intraparticle diffusion rate constant (mg g^{-1} $\text{min}^{-1/2}$). The plot of q_t vs. $t^{1/2}$ at different initial solution concentrations yields K_{int} and present multi-linearity indicating two or more steps occurring in the adsorption process. The first sharper portion indicates instantaneous adsorption. The second portion is the gradual adsorption stage with controlled intraparticle diffusion rate. The third step indicates the attainment of equilibrium stage where intraparticle diffusion starts to slow down due to enormously low concentration of solute in solution. The intraparticle diffusion rate is obtained from the slope of the gentle-sloped portion of the graph. The graphs present three stages of adsorption processes as can be observed from Fig. 6.

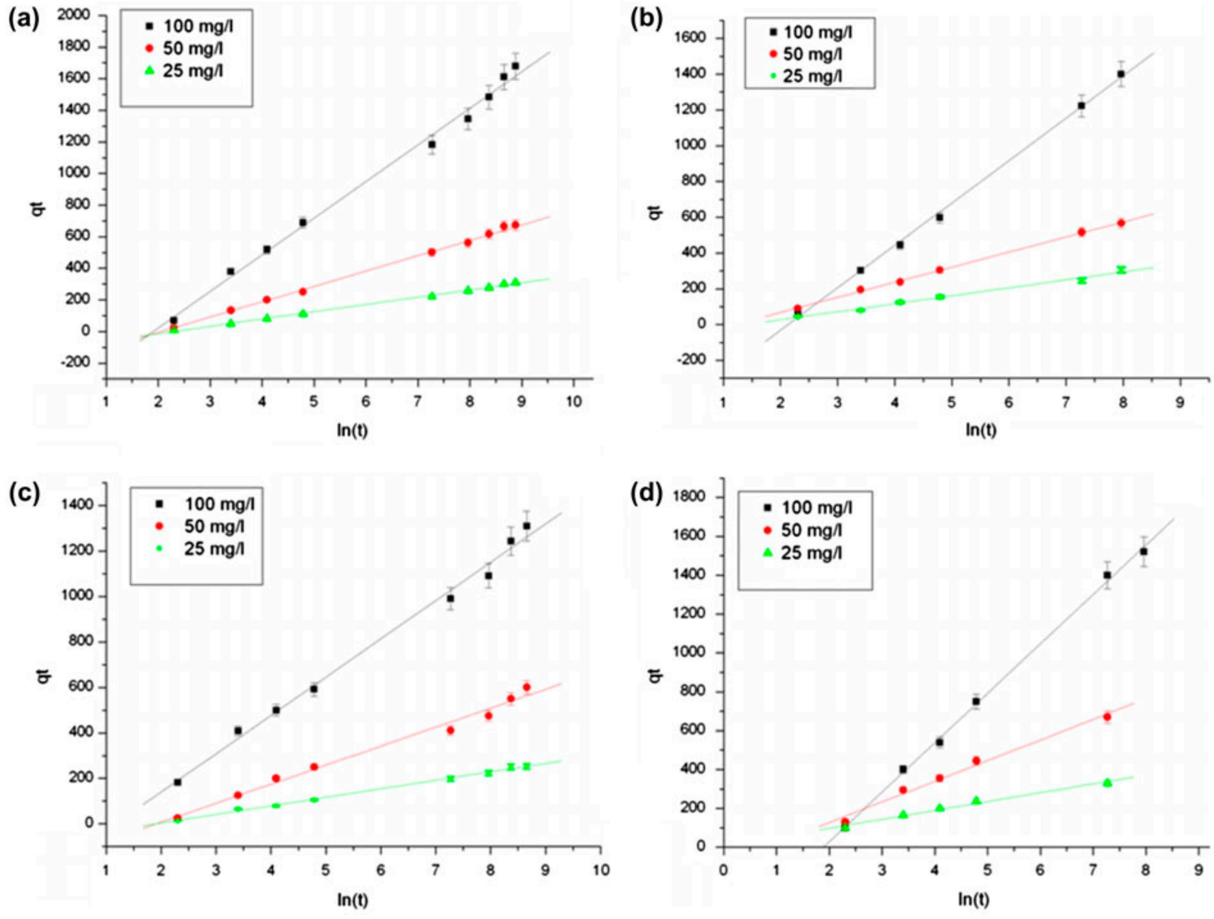

Fig. 5. Elovich model graphs for (a) *Phyllanthus emblica*, (b) *Mangifera indica*, (c) *Citrus limetta*, (d) *Citrus sinensis*.

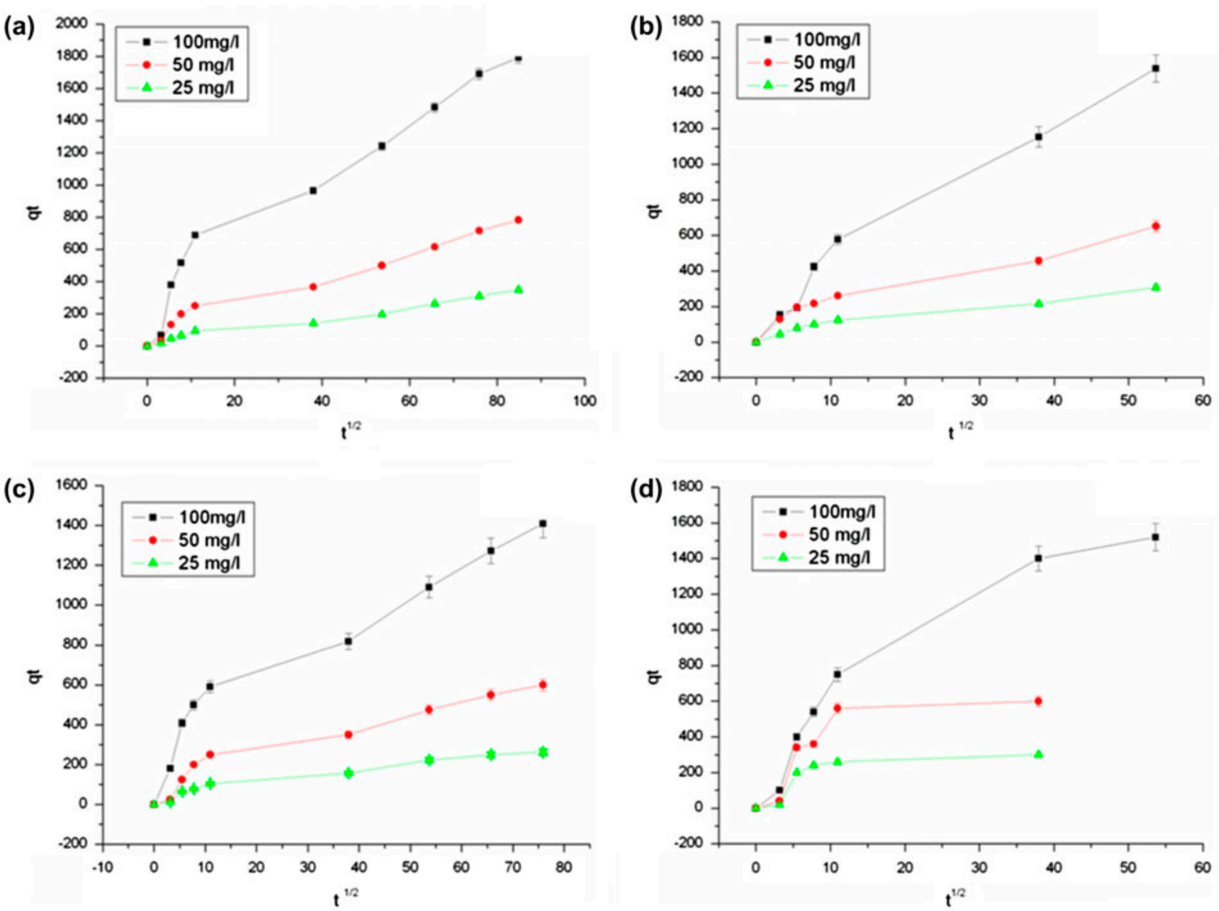

Fig. 6. Intraparticle diffusion model graphs for (a) *Phyllanthus emblica*, (b) *Mangifera indica*, (c) *Citrus limetta*, (d) *Citrus sinensis*.

The results suggest that the adsorption of Hg(II) ions from aqueous solution using the various citrus fruit waste peels followed the pseudo-first-order initially and the pseudo-second-order reaction mechanism at later stage.

3.5. Diffusion

During sorption of adsorbate in sphere of radius *r*, if the diffusion flux goes from regions of high concentration to regions of low concentration, with magnitude proportional to concentration (i.e. if the diffusion is fickian), the relation between weight uptake and sorption time is given as [65,66],

$$\frac{M_t}{M_\infty} = 6\left(\frac{Dt}{r^2}\right)^{\frac{1}{2}}\left[\pi^{\frac{1}{2}} + 2\sum_{n=1}^{\infty}\mathrm{ierfc}\left(\frac{nr}{\sqrt{Dt}}\right)\right] - 3\frac{Dt}{r^2} \tag{15}$$

(for short times)

$$\frac{M_t}{M_\infty} = 1 - \left(\frac{6}{\pi^2}\right)\sum_{n=1}^{\infty}\frac{1}{n^2}\exp\left(-\frac{\mathrm{D}n^2\pi^2 t}{r^2}\right) \tag{16}$$

(for moderate and long times)

where M_t and M_∞ are the weight uptake at time t and equilibrium, respectively. Eqs. (15) and (16) can be simplified to:

$$\frac{M_t}{M_\infty} = 6\left(\frac{D}{\pi r^2}\right)^{\frac{1}{2}} t^{\frac{1}{2}} \quad (\text{as}t \ll t_\infty) \tag{17}$$

$$\ln\left(1 - \frac{M_t}{M_\infty}\right) = \ln\left(\frac{6}{\pi^2}\right) + \left(\frac{-D\pi^2}{r^2}\right) \quad (\text{as } t < t_\infty) \tag{18}$$

It was found that the process of metal ion sorption occurs in two stages: first the external mass transport and second the intraparticle diffusion.

The external mass transport dominates in the early stage, while the intraparticle diffusion is the long-term stage of the experiment. The diffusion constant D_1 is calculated from the slope of straight line (0–30 min range) from the plot of M_t/M_∞ vs. $t^{1/2}$ using Eq. (17). The diffusion constant for long time D_2 can be calculated from the slope of the straight line of the plot of ln $(1-M_t/M_\infty)$ vs. t, using Eq. (18).

The variation in D_1 value with initial metal ions concentration is shown in Fig. 7(a). The D_1 values increased with increasing initial metal ion concentration in the concentration range from 25 to100 mg/L. Higher initial metal ion concentration has a higher concentration gradient which leads to an increase in the rate of ion diffusion.

The linear profiles for different solvents used could be found in the concentration range from 25 to 100 mg/L. The slope of the linear profiles for like *P. emblica*, *C. sinensis*, *C. limetta* and *M. indica* were 0.00952, 0.01416, 0.01367, and 0.0079, respectively. The results indicate the increase in the rate of diffusion in external mass transport resulting from the increased initial metal ion concentration. The values of D_1 for Hg(II) ions followed the following order: *C. sinensis*> *C. limetta* > *P. emblica* > *M. indica* indicating faster rate of diffusion for Orange and Indian Gooseberry peels than other citrus fruits.

The variation in D_2 value with change in initial metal ions concentration is shown in Fig. 7(b). The results indicated that value of D_2 remained constant with increasing initial Hg(II) ion concentration from 25 to 100 mg/L. The average value of D_2 for *C. sinensis*, *C. limetta*, *P. emblica* and *M. indica* was found to be 1.658×10^{-7}, 1.723×10^{-7}, 0.69×10^{-7} and 1.14×10^{-7} m^2/s, respectively.

The diffusion must pass through the adsorbed active sites located on a thin surface layer to reach the empty active sites located on the deeper layer of the adsorbent in the long-term stage. Therefore, the rate of ion diffusion in the intraparticle diffusion process is controlled by the ion diffusion in the adsorbent. The amount of adsorbed metal ions, on the active sites located on the thin surface layer as the initial metal ion concentration increases in the early stage, which leads to an increase in the disturbance during the pass-through for the diffusing ions and a resultant decrease in the rate of ion diffusion within the adsorbent. However, the rate of ion diffusion within the adsorbent would not vary with increasing initial metal ions concentration since the adsorbed active sites located on the thin surface layers were completely occupied by the metal ions during the early stage. The presence of capillaries plays an important role in intraparticle diffusion, as the upper layer get saturated with metal ions it gives the path for the Hg^{2+} ions to diffuse into the particle, hence increasing the rate of intraparticle diffusion (see Table 3).

3.6. Thermodynamic studies

Thermodynamic considerations are essential to decide the spontaneity in the adsorption process. The adsorption of Hg^{2+} ions on *P. emblica*, *C. sinensis*, *C. limetta* and *M. indica* was studied at 298 K. The free energy for adsorption (ΔG^o) was calculated from the equation [67]:

$$\Delta G^\circ = -RT \times \ln K_L \tag{19}$$

where K_L is the equilibrium constant obtained from Langmuir isotherm, R is universal gas constant (8.314 J mol^{-1} K^{-1}) and T is the absolute temperature (K). The free energy values obtained for uptake of Hg(II)

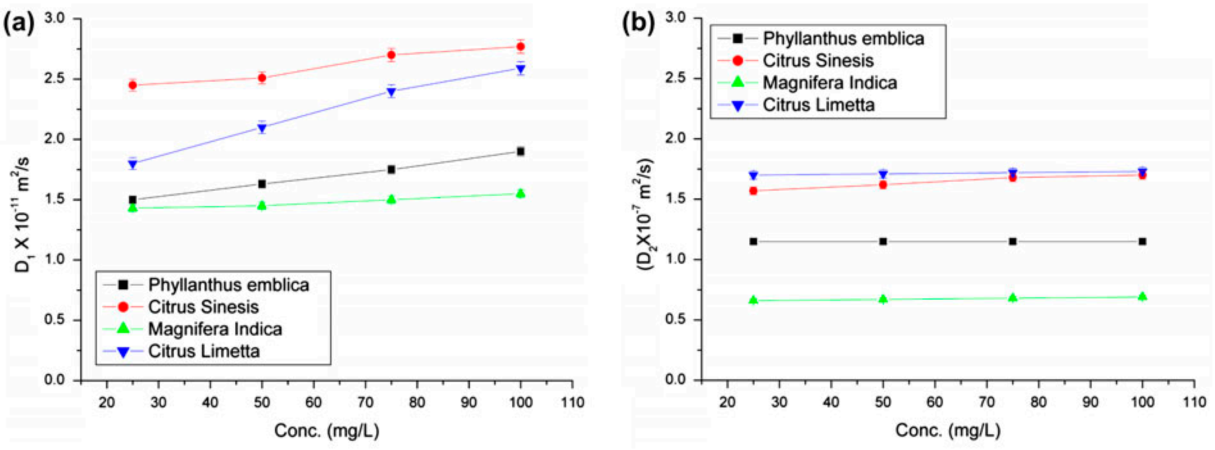

Fig. 7. Diffusion parameters for different sorbents (a) D_1 and (b) D_2.

Table 3
Kinetics parameters for Elovich and intra particle diffusion models

Adsorbents	Con. mg/L	Elovich $\sigma \times 10^{-3}$	q_σ	R^2	Intra particle diffusion K_{int}
Phyllanthus emblica	100	4.3118	0.1484	0.9939	19.218
	50	10.2955	0.1271	0.9902	8.384
	25	21.7350	0.1018	0.9975	3.740
Citrus limetta	100	4.2209	0.0848	0.9978	27.339
	50	11.8774	0.3055	0.9989	10.259
	25	22.3958	0.2439	0.9876	4.975
Mangifera indica	100	5.9379	0.3104	0.9927	15.791
	50	11.9879	0.1484	0.9862	7.201
	25	26.7101	0.1510	0.9968	3.256
Citrus sinensis	100	3.9316	0.1519	0.9984	27.620
	50	9.4153	0.4478	0.9872	13.696
	25	21.925	0.8573	0.9863	6.4775

ions onto *P. emblica*, *C. sinensis*, *C. limetta* and *M. indica* are −6.566, −9.519, −14.667, and −9.439 kJ mol^{-1}, respectively. The negative value obtained confirms feasibility, spontaneity and exothermic adsorption.

3.7. Desorption

The adsorbed Hg(II) ions finally precipitated and settled down along with the substrate particles. Hence, desorption of Hg(II) was not possible. These precipitated particles could be easily isolated by simple decantation process.

4. Conclusions

The experimental results obtained in this work demonstrates the possibility of using citrus fruit waste peels as a potential adsorbent for removal of Hg(II) ions from aqueous systems, especially in nations like India, Brazil and China where they are cultivated and contributed to a large amount to solid waste. Low cost citrus peels show an effective adsorption of 80% at pH 4. Initially, monolayer adsorption dominates the adsorption process as confirmed from the Langmuir isotherm followed by multi-layered adsorption indicted by Freundlich isotherm. The R_L values obtained ($0 < R_L < 1$) indicates favourable adsorption. But, both Langmuir and Freundlich isotherm models explains that the process of adsorption is Physico-chemical. The kinetic data agree very well with the pseudo-second-order adsorption mechanism and the rate is diffusion controlled. The intraparticle diffusion model reveals multistep diffusion process with slow state diffusion. Diffusion follows the Fick's law. D_1 values for Hg(II) ions following the order *Phyllanthus emblica* > *C. sinensis* > *C. limetta* > *M. indica* indicating faster rate of diffusion for (*P. emblica* and *C. sinensis*) than others. Both Fick's and intraparticle diffusion are observed with these citrus peels with capillarity action playing an important role in slow and controlled diffusion of Hg(II) ions. Also, the antioxidant properties of citrus peels especially due to the presence of ascorbic acid was found to be effective in reducing and binding the Hg(II) ions on the sorbents as confirmed from the XRD data. The interactions of sulphur groups present in the citrus fruit peels with the Hg(II) ions enhanced the metal ion adsorption. These interactions are indicated by the formation of silvery-black precipitate after 4 days of contact time. The thermodynamic study reveals the spontaneous and exothermic adsorption. Thus, this technique proves to be highly cost-effective and eco-friendly since waste fruit peels are used to remove the toxic heavy metal ions.

Acknowledgements

The authors thank Dr Prahlada (Vice Chancellor, DIAT(DU)) for the support and help he extended to us in the research activities and Prof Om Parkash (Head of Department, Ceramic Engineering, IIT (BHU), Varanasi) for helping us in getting the internship and thereby, giving us the opportunity to work at DIAT. We would also thank Dr Renuka Gonte, DIAT and Vivek Verma IISER Pune for their continued technical support.

References

[1] W.F. Fitzgerald, D.R. Engstrom, R.P. Mason, E.A. Nater, The case for atmospheric mercury contamination in remote areas, Environ. Sci. Tchnol. 32(1) (1998) 1–7.

[2] E.P.A., National Primary Drinking Water Regulations, 40 CRF Ch.I (7- 1-02 ed.), US Environmental Protection Agency (EPA), Washington, DC, 2002. Available from: http://www.acess.gpo.gov/nara/cfr/waisidx 02/40 cfr141 02.html

[3] J.A. Ritter, J.P. Bibler, Removal of mercury from waste water: Large-scale performance of an ion exchange process, Water Sci. Technol. 25 (1992) 165–172.

[4] X.W. Wu, H.W. Ma, J.H. Li, J. Zhang, Z.H. Li, The synthesis of mesoporous aluminosilicate using microline for adsorption of mercury(II), J. Colloid Interface Sci. 315 (2007) 555–561.

[5] S.X. Li, Z. Feng-Ying, H. Yang, N. Jian-Cong, Thorough removal of inorganic and organic mercury from aqueous solutions by adsorption on lemna minor powder, J. Hazard. Mater. 186 (2011) 423–429.

[6] M. Aschner, J.L. Aschner, Mercury neurotoxicity: Mechanisms of blood-brain barrier transport, Neurosci. Biobehav. Rev. 14(2) (1990) 169–176.

[7] C. Namasivayam, K. Kadirvelu, Uptake of mercury(II) from waste water by activated carbon from an unwanted agricultural solid by-product: Coirpith, Carbon 37 (1999) 79–84.

[8] M. Harada, Minamata disease: Methylmercury poisoning in Japan caused by environmental pollution, Crit. Rev. Toxicol. 25 (1995) 1–24.

[9] M. Harada, Neurotoxicity of methylmercury: Minamata and the Amazon. in: M. Yasui, M.J. Strong, K. Ota, M.A. Verity (Eds.), Mineral and Metal Neurotoxicology. CRC Press, Boca Raton, FL, 1997, pp. 177–188.

[10] M. Harada, Characteristics of industrial poisoning and environmental contamination in developing countries, Environ. Sci. 4 (1996) 157–169.

[11] K.A. Krishnan, T.S. Anirudhan, Removal of mercury (II) from aqueous solutions and chlor-alkali industry effluent by steam activated and sulphurised activated carbons prepared from bagasse pith: Kinetics and equilibrium studies, J. Hazard. Mater. 92 (2002) 161–183.

[12] E.I. El-Shafey, Removal of Zn(II) and Hg(II) from aqueous solution on a carbonaceous sorbent chemically prepared from rice husk, J. Hazard. Mater. 175 (2010) 319–327.

[13] Mercury in India Usage and Releases, Available from: http://www.toxicslink.org/docs/06035_publications-1-33-2.pdf

[14] University of Wisconsin-Madison, Mercury Pollution Threatens Health Worldwide, Scientists Say, Science Daily, 2006, August 11.

[15] M.M. Matlock, B.S. Howerton, D.A. Atwood, Chemical precipitation of lead from lead battery recycling plant wastewater, Ind. Eng. Chem. Res. 41 (2002) 1579–1582.

[16] M.E. Paaez-Hernandez, K. Aguilar-Argteaga, C.A. Galaan-Vidal, M. Palomar-Pardavea, Mercury ions removal from aqueous solution using an activated composite membrane, Environ. Sci. Technol. 39 (2005) 7667–7670.

[17] A. Dabrowski, Z. Hubicki, P. Podkoscielny, E. Robens, Selective removal of the heavy metal ions from waters and industrial wastewaters by ion-exchange method, Chemosphere 56 (2004) 91–106.

[18] H. Agarwal, D. Sharma, S.K. Sindhu, S. Tyagi, S. Ikram, Removal of mercury from wastewater use of green adsorbents—a review, Electron. J. Environ. Agric. Food Chem. 9(9) (2010) 1551–1558.

[19] C.J. Moon, J.H. Lee, Use of curdlan and activated carbon composed adsorbents for heavy metal removal, Process Biochem. 40 (2005) 1279–1283.

[20] N. Feng, X. Guo, S. Liang, Y. Zhu, J. Liu, Biosorption of heavy metals from aqueous solutions by chemically modified orange peel, J. Hazard. Mater. 185 (2011) 49–54.

[21] M.A. Barakat, New trends in removing heavy metals from industrial wastewater, Arabian J. Chem. 4 (2011) 361–377.

[22] X. Ying, Z. Fang, Experimental research on heavy metal wastewater treatment with dipropyl dithiophosphate, J. Hazard. Mater. B-137 (2006) 1636–1642.

[23] L.B. Khalil, M.W. Rophael, W.E. Mourad, The removal of the toxic Hg(II) salts from water by photocatalysis, Appl. Catal. B: Environ. 36 (2002) 125–130.

[24] C. Miranda, J. Yãnez, D. Contreras, R. Garcia, W.F. Jardim, H.D. Mansilla, Photocatalytic removal of methylmercury assisted by UV-A irradiation, Appl. Catal. B: Environ. 90 (2009) 115–119.

[25] B. Volexy, Detoxification of metal-bearing effluents: Biosorption for the next century, Hydromettalurgy 59 (2001) 203–216.

[26] A.I. Zouboulis, M.X. Loukidou, K.A. Matis, Biosorption of toxic metals from aqueous solutions by bacteria strains isolated from metal polluted soils, Process Biochem. 39 (2004) 909–916.

[27] A. Hutchison, D. Atwood, Q.E. Santillian-Jiminez, The removal of mercury from water by open chain ligands containing multiple sulfurs, J. Hazard. Mater. 156 (2008) 458–465.

[28] M.H. Ansari, A.M. Deshkar, P.S. Kelkar, D.M. Dharmadhikari, M.Z. Hasan, R. Paramasivam, Mercury removal from water by steamed hoof powder, Water Sci. Technol. 40 (1999) 109–116.

[29] S. Kushwaha, B. Shreedhar, P.P. Sudhakar, Adsorption of Hg2+ onto Borassus flabeliffer: A redox mechanism, Chem. Eng. J. 193–194 (2012) 328–338.

[30] D.P. Tiwari, D.K. Singh, D.N. Saxena, Hg(II) adsorption from aqueous solutions using rice husk ash, J. Environ. Eng. 121 (1995) 470–481.

[31] T. Kiyohara, K. Anazawa, H. Sakamoto, T. Tomiyasu, Adsorption of mercury on used tea leaves and coffe beans, Bunseki Kagaku 52 (2003) 887–890.

[32] X. Ma, K.S. Subramanian, C.L. Chakrabarti, R. Guo, J. Cheng, Y. Lu, W.F. Pickering, Removal of trace mercury(II) from drinking water: Sorption by granular activated carbon, Environ. Sci. Health 27 (1992) 1389–1404.

[33] W.R. Knocke, L.H. Hemphill, Mercury (II) sorption by waste rubber, Water Res. 15 (1981) 275–282.

[34] M.K. Sreedhar, A. Madhukumarand, T.S. Anirudhan, Evaluation of an adsorbent prepared by treating coconut husk with polysulphide for the removal of mercury from wastewater, Indian J. Eng. Mater. Sci. 6 (1999) 279–285.

[35] S.K. Srivastava, R. Tyagi, N. Pant, Adsorption of heavy metal ions on carbonaceous material developed from the waste slurry generated in local fertilizer plants, Water Res. 23 (1989) 1161–1165.

[36] C. Namasivayam, K. Periasamy, Bicarbonate-treated peanut hull carbon for mercury(II) removal from aqueous solution, Water Res. 27 (1993) 1163–1168.

[37] B.S. Inbaraj, N.S. Sulochana, Utilisation of an agricultural waste jack fruit peel for the removal of Hg(II) from aqueous solution. in: R.L. Mersky (Ed.) Proceeding of 17th International Conference on Solid Waste Technology and Management, Philadelphia, 2001, pp. 802–811.

[38] C. Namasivayam, K. Kadirvelu, Uptake of mercury (II) from wastewater by activated carbon from an unwanted agricultural solid by-product coirpith, Carbon 37 (1999) 79–84.

[39] M. Cox, E.I. El-Shafey, A.A. Pichugin, Q. Appleton, Removal of mercury (II) from aqueous solution on a carbonaceous sorbent prepared from flax shive, Chem. Technol. Biotechnol. 75 (2000) 427–435.

[40] K. Kadivelu, M. Kavipriya, C. Karthika, N. Vennilamani, S. Pattabhi, Mercury(II) adsorption by activated carbon made from sago waste, Carbon 42 (2004) 745–752.

[41] A.C. Barbosa, A.A. Boischio, G.A. East, I. Ferrari, A. Gonçalves, P.R.M. Silva, T.M.E. da Cruz, Mercury contamination in the Brazilian Amazon. Environmental and occupational aspects, Water Air Soil Pollut. 80 (1–4) (1995) 109–121.

[42] F.A. Pavan, I.S. Lima, E.C. Lima, C. Aroldi, Y. Gushikem, Use of Ponkan mandarin peels as biosorbent for toxic metals uptake from aqueous solutions, J. Hazard. Mater. B137 (2006) 527–533.

[43] W.L. McCabe, J.C. Smith, P. Harriott, Unit Operations of Chemical Engineering. 5th ed., McGraw-Hill Publishers, International Editions, 1993. ISBN 0-07-044844-2.

[44] A.Y.Y. Loo, Y.P. Lay, M.G. Kutty, O. Timpe, M. Behrens, S.B.A. Hamid, Spectrophotometric determination of mercury with iodide and rhodamine B, Sains Malaysiana 41(2) (2012) 213–218.

[45] J. Bassett, R.C. Denney, G.H. Jeffery, J. Mendhan, Vogel's Textbook of Quantitative Inorganic Analysis including Elementary Instrumental Analysis. fourth ed, Longman Group Limited, 1982. ISBN 0-582-40710-9.

[46] B.S. Inbaraj, N. Sulochna, Mercury adsorption on a carbon sorbent derived from fruit shell of Terminalia catappa, J. Hazard. Mater. 133 (2006) 283–290.

[47] R. Gonte, K. Balasubramanian, Heavy and toxic metal uptake by mesoporous hypercrosslinked SMA beads: Isotherms and kinetics, J. Saudi Chem. Soc. (2013), doi: http://dx.doi.org/10/1016/j.jscs.2012.04.003

[48] Z. Aksu, Determination of the equilibrium, kinetics and thermodynamic parameters of the batch biosorption on nickel (II) ions onto Chlorella vulgaris, Process Biochem. 38 (2002) 89–99.

[49] I. Langmuir, The constitution and fundamental properties of solids and liquids, J. Am. Chem. Soc. 38 (11) (1916) 2221–2295.

[50] Y. Zhang, Y. Li, X. Li, L. Yang, X. Bai, Z. Ye, L. Zhou, L. Wang, Selective removal of Pb^{2+} in aqueous environment by using novel macroreticular PVA beads, J. Hazard. Mater. 181 (2010) 898–907.

[51] K.R. Hall, L.C. Eagleton, A. Acrivos, T. Vermeulen, Pore and solid diffusion kinetics in fixed bed adsorption under constant—pattern condition, Ind. Eng. Chem. Fundam. 5 (1996) 212–223.

[52] A. Benhamou, M. Baudu, Z. Derriche, J.P. Basly, Aqueous heavy metal removal on amine functionalized Si-MCM and Si-MCM-48, J. Hazard. Mater 171 (2009) 1001–1008.

[53] Y.H. Li, Z. Di, J. Ding, D. Wu, Z. Luan, Y. Zhu, Adsorption thermodynamic, kinetic and desorption studies of Pb^{2+} on carbon nanotubes, Water Res. 39 (2005) 605–609.

[54] R. Djeribi, O. Hamdaoui, Sorption of copper(II) from aqueous solution by cedar sawdust and crushed brick, Desalination 225 (2008) 95–112.

[55] G.D. Halsey, The role of surface heterogeneity, Adv. Catal. 4 (1952) 259–269.

[56] K.K.H. Choy, G. McKay, J.F. Porter, Sorption of acid dyes from effluents using activated carbon, Resour. Conserv. Recycl. 27 (1999) 57.

[57] P.A. Kumar, M. Ray, S. Chakraborty, Adsorption behaviour of trivalent chromium on the amine—based polymer aniline formaldehyde condenstate, Chem. Eng. J. 149 (2009) 115–127.

[58] B. Kiran, A. Kaushik, Chromium binding capacity of Lyngbya putealis exopolysaccarides, Biochem. Eng. J. 38 (2008) 47–54.

[59] S. Rengaraj, J.-W. Yeon, Y. Kim, Y. Jung, Y.-K. Ha, W.-H. Kim, Adsorption characteristics of Cu(II) onto ion exchange resins 252H and 1500H: Kinetics, isotherms and error analysis, J. Hazard. Mater. 143 (2007) 469–477.

[60] Y. Sag, Y. Aktay, Kinetic studies on sorption of Cr(VI) and Cu(II)ions by chitin, chitosan and Rhizopus arrhizus, Biochem. Eng. J. 12 (2002) 143–153.

[61] A. Gunay, E. Arslankaya, I. Tosun, Lead removal from aqueous solution by natural and pretreated clinoptilolite: Adsorption equilibrium and kinetics, J. Hazard. Mater. 146 (2007) 362–371.

[62] O. Hamdaoui, M. Chiha, Removal of methylene blue from aqueous solutions by wheat bran, Acta Chim. Slov. 54 (2007) 407–418.

[63] M. Sarkar, P.K. Acharya, B. Battacharya, Modeling the adsorption kinetics of some priority organic pollutants in water from diffusion and activation energy parameters, J. Colloid Interface Sci. 266 (2003) 28.

[64] W.J. Weber, J.C. Morris, Kinetics of adsorption on carbon from solution, J. Sanit. Eng. Div. Am. Soc. Civ. Eng. 89 (1963) 31.

[65] J. Crank, The Mathematics of Diffusion. 2nd ed., Clarendon, Oxford, 1975.

[66] J. Crank, G.S. Park, Diffusion in Polymers, Academic, London, 1968.

[67] Y.S. Al-Dengs, M.I. El-Barhhouthi, A. El-Shaikh, G. Walker, Effect of solution pH, ionic strength and temperature on adsorption behaviour of reactive dyes on activated carbon, Dyes Pigm. 77 (2007) 16–23.